Characterization of oxidative stress in Leishmaniasis-infected or LPS-stimulated macrophages using electrochemical impedance spectroscopy

Karine Reybier[a,c,*,1], Clotilde Ribaut[a,c,1], Agnès Coste[a,c], Jérôme Launay[d], Paul Louis Fabre[b], Françoise Nepveu[a,c]

[a] *Université de Toulouse, UPS, LPSNPR (Laboratoire pharmacochimie des substances naturelles et pharmacophores redox), 118, route de Narbonne, F-31062 Toulouse cedex 9, France*
[b] *Université de Toulouse, UPS, INP, CNRS, LGC (Laboratoire de Génie Chimique), F-31062 Toulouse, France*
[c] *IRD, LPSNPR, F-31062 Toulouse, France*
[d] *CNRS, UPS, INSA, LAAS (Laboratoire d'Analyse et d'Architecture des Systèmes), F-31077 Toulouse, France*

A B S T R A C T

The physiological changes caused by external stimuli can be employed as parameters to study pathogen infection in cells and the effect of drugs. Among analytical methods, impedance is potentially useful to give insight into cellular behavior by studying morphological changes, alterations in the physiological state, production of charged or redox species without interfering with *in vitro* cellular metabolism and labeling. The present work describes the use of electrochemical impedance spectroscopy to simply monitor by modeling impedance plots (Nyquist diagram) in appropriate equivalent circuit, the changes affecting murine macrophage cell line (RAW 264.7) in response to parasite infection by *Leishmania amazonensis* or to lipopolysaccharide (LPS) treatment. These results demonstrate the ability of electrochemical impedance spectroscopy to discriminate between two opposite cell responses associated to two different stimuli, one caused by the internalization of a parasite, and the other by activation by a bacterium component. Indeed, the study has allowed the characterization, from an electrical point of view, of the extra-cellular NO radical produced endogenously and in great quantities by the inducible form of NO-synthase in the case of LPS-stimulated macrophages. This production was not observed in the case of *Leishmania*-infected macrophages for which to survive and multiply, the parasite itself possesses mechanisms which may interfere with NO production. In this latest case, only the intracellular production of ROS was observed. To confirm these interpretations confocal microscopy analysis using the ROS (reactive oxygen species) fluorescent probe 2′,7′-dichlorodihydrofluorescein diacetate and electron paramagnetic resonance experiments using $Fe(DETC)_2$ as NO radical spin trap were carried out.

1. Introduction

Cells represent the minimum functional and integrating communicable units of living systems. During their life cycle they act both as transducers and transmitters of various chemical and physical signals through the production of specific molecules. The physiological changes caused by external stimuli might be employed as parameters to study pathogen infection in cells, and the effect of drugs. Cell-based sensors are new hybrid systems using the abilities of the cell to detect, transduce and amplify small changes originating from stimuli (McFadden, 2002; Stenger et al., 2001). These assays offer a significant range of opportunities based on the ability of cells to recognize a broad range of biologically active substances affecting their response. Cell-based biosensors have been implemented for a number of applications ranging from pharmaceutical screening (Asphahani and Zhang, 2007), to detection of environmental pollutants (Pinsino et al., 2008) or pathogens (bacteria and viruses) (Rider et al., 2008). Applications are very dependent on the transduction mode which can be electric, optic or even piezoelectric or a combination of different types (De Blasio et al., 2004), and to cell types including macrophages (Kowolenko et al., 1990), fibroblasts (Tlili et al., 2003; Xiao and Luong, 2005), epithelial and endothelial (Marx et al., 2005) cells. Among cellular biosensors, impedance cell-based sensor arrays which were first described by Giaever and Keese (1984), are potentially useful to give insight into cellular behavior, to detect morphological changes (Arndt et al., 2004), to study cell adhesion (De Blasio et al., 2004), attachment and spreading (Luong et al., 2001; Xiao et al., 2002), alterations in the physiological state or to test the efficiency of drugs

* Corresponding author at: Université de Toulouse, UPS, Faculté des sciences pharmaceutiques, 118, route de Narbonne, F-31062 Toulouse cedex 9, France.
Tel.: +33 5 62259804.
E-mail address: reybier@cict.fr (K. Reybier).
[1] These authors contributed equally to the work.

(Otto et al., 2004) or effectors (Nguyen et al., 2004; Tiruppathi et al., 1992; Tlili et al., 2003). The physical background to the technique is based on the electrically insulating effect of cell membranes at low frequencies. The cellular sensing method allows real-time monitoring of cells, avoids the use of labeled molecules and does not interfere with *in vitro* cellular metabolism. Even if cellular biosensors have been applied in many different fields, the literature on cell-based devices involving two living entities, such as a parasite developing in its host cell, is very rare.

Leishmaniasis is an infectious disease caused by intracellular protozoa from the genus *Leishmania* affecting over 12 million people worldwide. After entry into its mammalian host, *Leishmania* is phagocytosed by macrophages and confined to a lysosome-like compartment, known as the parasitophorous vacuole (Russell, 1995), where it develops and proliferates. When parasites are numerous enough, *i.e.* after 20–30 h, the macrophage disrupts and releases amastigotes internalized by new naive macrophages. Hence, the macrophage constitutes both the host and the effector cell against *Leishmania* infections (Ritting and Bogdan, 2000). Furthermore, the macrophage possesses a number of primary defence mechanisms against microbial pathogens, including the production of reactive oxygen intermediates (ROIs) and reactive nitrogen intermediates (RNIs). *Leishmania* promastigotes have been shown to be susceptible to both ROIs and RNIs.

The aim of the present work is to use electrochemical impedance spectroscopy (EIS) to simply monitor changes from an electrical point of view, and in particular oxidative stress generated by murine macrophage cell line RAW 264.7 in response to parasite infection by *Leishmania amazonensis* (*L. amazonensis*) or to lipopolysaccharide (LPS) (Stuehr and Marletta, 1987) treatment. Identification of morphological changes and oxidative events taking place in macrophages during activation by *Leishmania* could help in the comprehension of infectious mechanisms to fight this neglected disease which has only a few efficient treatment drugs, most of them being very toxic.

2. Materials and methods

2.1. RAW 264.7 cell culture

RAW 264.7 cells were cultivated in Dulbecco's Modified Eagle Medium (DMEM, Gibco BRL) supplemented with sodium bicarbonate (1.5 g/L; Lonza), D-(+)-glucose (4.5 g/L; Sigma–Aldrich), L-glutamine (4 mM; Lonza) and 10% decomplemented foetal bovine serum (Lonza). The cells were maintained at 37 °C in a 5% CO_2 atmosphere.

2.2. Parasites and in vitro cultures

Promastigote cultures were derived from axenically grown amastigote stages by subpassage at 25 ± 1 °C in medium RPMI 1640 (Roswell Park Memorial Institute medium, Lonza) buffered with 25 mM HEPES (4-(2-hydroxyethyl)-1-piperazineethanesulfonic acid, Lonza) and 2 mM $NaHCO_3$ (Sigma–Aldrich), pH 7.2, supplemented with 20% heat-inactivated foetal bovine serum (FBS, Lonza), 2 mM L-glutamine, 100 U/mL penicillin and 100 μg/mL streptomycin (Gibco, BRL). Promastigote cultures were maintained at 25 ± 1 °C in RMPI 1640 supplemented with 10% of decomplemented FBS.

2.3. In vitro RAW 264.7 cell infection or activation

The macrophage murine cell line RAW 264.7 was maintained in an exponential growth phase by subsequent splitting in DMEM complemented with 10% of FBS. RAW 264.7 cells were infected with promastigote at a parasites: macrophage ratio of 5:1 for 1 h at 37 °C with 5% CO_2. Non-internalized parasites were removed by gently washing in pre-warmed PBS.

RAW 264.7 were activated with LPS at 1 or 10 μg/mL (stock solution at 1 mg/mL in sterile EBSS (Earle's Balanced Salt Solution)) depending on experiments, for 1 h at 37 °C with 5% CO_2. The culture was then rinsed with pre-warmed PBS.

2.4. Confocal microscopy

The macrophage murine cell line RAW 264.7 was cultured on a Lab-Tek chamber slide and was infected or stimulated as describe above. Non-adhesive cells were removed by washing in pre-warmed PBS. The fixed cells were incubated with 2′,7′-dichlorofluorescein diacetate (20 μM; Sigma–Aldrich), for 20 min at 37 °C and 5% CO_2 (Kondo et al., 2001). A confocal laser-scanning microscope (LSM 510, Zeiss) was used to visualize the production of radical species such as $RO^{\bullet}$, $ROO^{\bullet}$, $^{\bullet}NO_2$, $CO^{\bullet}{}_3$, $^{\bullet}OH$ and NO.

2.5. EPR experiments

Electron paramagnetic resonance spectroscopy (EPR) experiments were carried out for RAW cells activated with LPS and infected with *L. amazonensis*, as described above. The cells were then incubated in DMEM containing 3% (w/w) bovine albumin, NaDETC (sodium diethyldithiocarbamate, 2 mM; Sigma–Aldrich), and $FeSO_4$ (1 mM; Sigma–Aldrich) at 37 °C and 5% CO_2. After 2 h of incubation, 300 μL of supernatant was placed in a quartz EPR tube (inner diameter 4 mm) for EPR analysis. X-band EPR spectra were obtained at 112 K on a Bruker EMX-8/2.7 (9.86 GHz) equipped with a high-sensitivity cavity (4119/HS 0205) (Bruker, Wissembourg, France) and a teslameter (Bruker ER 0.35). Processing of EPR data was performed using WINEPR software (Bruker). Typical scanning parameters were: scan number, 5; modulation amplitude, 5 G; modulation frequency, 100 kHz; microwave power, 20.12 mW; time constant, 10.24 ms; receiver gain: 2×10^4.

2.6. Electrode manufacturing process and electrode modification

Firstly, P-type (3–5 $\Omega\,cm^{-1}$) silicon substrates were thermally oxidized to grow an 800 nm thick silicon oxide SiO_2 layer. A titanium/gold deposit (30 nm/300 nm) was then performed by evaporation at low deposit rates (1 nm/min).

The gold electrodes were firstly washed in a piranha mixture (70% H_2SO_4/30% H_2O_2; Sigma–Aldrich) for 3 min. Electrode modification by cells was carried out by re-suspending adherent RAW cells in a flask whose bottom had been covered by the electrodes (gold faces up) at 37 °C in a 5% CO_2 atmosphere for 24 h.

2.7. Electrochemical impedance spectroscopy

Electrochemical experiments were performed at 25 °C using a Voltalab 80 PGZ 402 with a three-electrode cell including a calomel electrode as the reference electrode, a gold electrode (0.255 cm^2) as the counter electrode and a modified gold electrode (0.053 cm^2) as the working electrode. EIS with a chemical probe $[Fe(CN)_6]^{3-/4-}$ (1:1) (5 mM, Sigma–Aldrich) was carried out in PBS solution (pH 7.4), while EIS without chemical probe was performed in the culture medium. Impedance spectra were recorded in a free-potential frequency range from 50 kHz to 100 mHz The amplitude of the alternating voltage was 10 mV. Impedance experiments were done in quadruplate for a same culture.

3. Results and discussion

Impedance biosensors are based on electrochemical impedance spectroscopy (EIS) which measures the electrical impedance of an

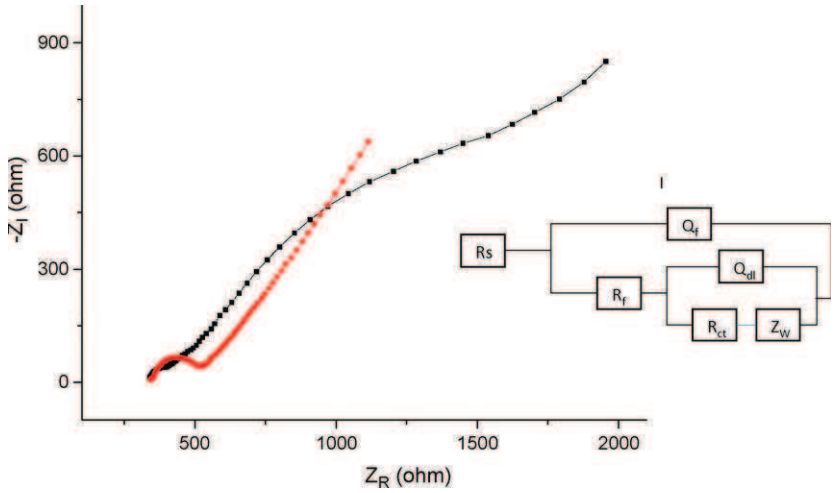

Fig. 1. Influence of cellular layer on impedance response. Nyquist impedance plots in the frequency range 50 kHz to 100 mHz obtained in the presence of 5 mM $Fe(CN)_6^{3-/4-}$ (1:1) in PBS with (■) a bare gold electrode and (●) a gold electrode modified with macrophages, the symbols correspond to experimental data and the line represents the simulated spectra with the parameters calculated by FRA software from the equivalent circuit model I.

interface by imposing or not (free potential) a small sinusoidal voltage and measuring the resulting current at different frequencies. Impedance Z is given by the ratio voltage–current. From the Nyquist plots, *i.e.* $-Z_{\text{imaginary}} = f(Z_{\text{real}})$ recorded for different frequencies it is possible, by modeling, to convert the interface in equivalent circuits (composed of resistances and capacities) taking into account electronic transfer and mass diffusion which takes place at the cell/solution interface. Among EIS experiments, two methods exist. EIS using a redox couple as a probe ($Fe(CN)_6^{3-/4-}$, for example), to characterize the electrode surface by determining kinetic parameters and the surface coverage after modification, and EIS carried out probe-free, which gives information about species produced by the covering layer. In our case EIS was applied to gold electrodes modified by infected or stimulated macrophages.

3.1. Characterization of the cellular layer by EIS using a redox probe

Impedance measurements were carried out at the free potential of the electrode with an equimolar mixture of potassium ferrocyanide/ferricyanide as redox probe. The Nyquist diagrams, corresponding to the gold electrode before and after modification with RAW cells, are presented in Fig. 1. In all cases, the curves highlight a semicircle immediately followed by the Warburg line, whose slope is equal to unity. The semicircle characterizes the electron transfer and Warburg line mass transfer. It can be noted that the presence of RAW cells at the gold surface induces an increase in the semicircle diameter resulting from the insulating properties of the cells.

In order to obtain kinetic parameters of the film, Nyquist plots were fitted according to circuit model I presented in Fig. 1 (Ribaut et al., 2009). The electrochemical system is described by the standard Randles circuit: as usual, R_s is the electrolyte resistance, Q_{dl} the double-layer capacity (here a constant phase element (CPE)), R_{ct} the charge transfer resistance and Z_w the Warburg impedance under non-stationary conditions, characterized by the Warburg coefficient σ with $Z_w = \sigma/\omega^{1/2} - j\sigma/\omega^{1/2}$ and $\omega = 2\pi f$.

The cellular layer is taken into account by to the typical Randles circuit, of R_f, film resistance and Q_f, dielectric capacitance corresponding to the film.

Electric-component values deduced from modeling are presented in Table 1. The increase in charge transfer resistance is related to electrode coverage θ by the relationship $1 - \theta = R_{ct}^0/R_{ct}$ where θ is the apparent electrode coverage, assuming that all the current passes through bared spots on the electrode, R_{ct}^0 the charge transfer resistance measured at the bare Au electrode and R_{ct} the charge transfer resistance measured under the same conditions at the modified electrode. From R_{ct}^0 and R_{ct} given in Table 1, the electrode coverage θ is equal to $93 \pm 2\%$. The presence of the film implies the addition of an imperfect capacitance Q_f for which n, which characterizes inhomogeneities (surface roughness, $0 < n < 1$) of the analyzed layer, equals to 0.7. This value is relatively weak revealing a rough surface due to the cell monolayer.

As shown in Table 1, the macrophages layer on the gold surface leads to a 80-fold increase in the double-layer capacity. This increase may result from the fact that cellular plasmatic membranes are coated with an external layer containing negatively charged polysaccharides (Mutsaers and Papadimitrou, 1988). The presence of negative charges on the surface, induces with positive charges available in the electrolyte, a large charge separation responsible for the high value recorded for Q_{dl}.

3.2. Characterization by EIS of the cellular layer after infection by Leishmania or stimulation with LPS

Impedance spectroscopy measurements, with or without use of a probe, were carried out on healthy, *Leishmania*-infected and LPS-stimulated RAW macrophages. The corresponding plots are presented in Fig. 2. The corresponding plots clearly highlight great differences between the three cell states. In order to obtain information on the electrical properties of parasitized or stimulated versus normal macrophages, impedance plots corresponding to measurement completed with a probe were fitted according to the model circuit I presented in Fig. 1. However, in the case of EIS carried out without probe, the modeling did not provide satisfactory fitting with experimental data. This difficulty may come from reactive-species production within the macrophage itself, thus rendering the equivalent circuit inappropriate; this production is masked when experiments are carried out with a redox probe. Indeed, to kill intra- and extra-cellular parasites, various oxidant-generating enzymes are activated among which NADPH oxidase and xanthine oxidase, leading to the production of superoxide anion and inducible nitric oxide synthase (iNOS), which produces nitric oxide (Gantt et al., 2001; Lemesre et al., 1997; Mehta and Shaha, 2006). For this reason, circuit model II presented in Fig. 2 was preferred to circuit model I given in Fig. 1. This circuit includes in series a charge transfer resistance R_{ads} and a capacitance C_{ads} which take

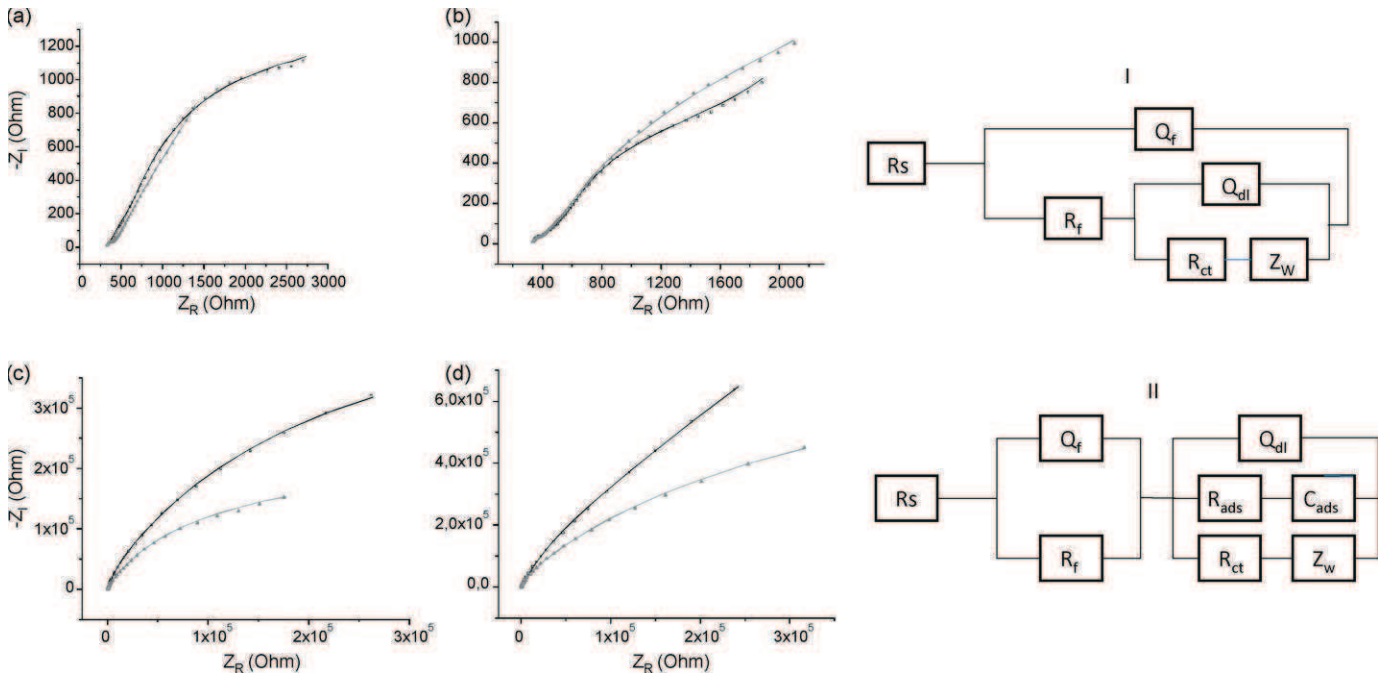

Fig. 2. Influence of the macrophage state, *Leishmania*-infected or LPS-stimulated, on the EIS measurements. Nyquist impedance plots in the frequency range 50 kHz to 100 mHz obtained in the presence of 5 mM $Fe(CN)_6^{3-/4-}$ (1:1) in PBS (a and b) or in the culture medium (c and d) with a gold electrode modified with (□) healthy, (▲) *Leishmania*-infected (a and c) or LPS-stimulated macrophages (b and d). The symbols correspond to experimental data and the line represents simulated spectra with parameters calculated by FRA software from equivalent circuit model I (for a and b) or II (for c and d).

into account redox species production in the cellular layer. R_{ads} corresponds to a charge transfer resistance whereas C_{ads} represents the concentration of adsorbed electroactive species.

The value of the components deduced from modeling with circuit models I or II, respectively, for EIS performed with or without probe, are detailed in Table 1. The comparison between values deduced from experiments carried with or without redox probe facilitates interpretation of the events induced by pathogen infection or LPS stimulation. It is important to mention that the control values from non-infected and non-stimulated macrophages change with each experiment because the same RAW cell line, but not in the same passage number, was used. With an increasing passage number, the cells can change morphologically, and phenotypic variations can appear leading to great variations in component values deduced from modeling as an equivalent circuit.

Electrolyte resistance is logically constant independently of the cellular state with a value equal to 330 Ω for experiments carried out with $[Fe(CN)_6]^{3-/4}$. In the case of experiments performed in the culture medium, R_s is almost constant (450 Ω) with a very weak increase in the case of LPS-stimulated macrophages.

Concerning film characteristics, *i.e.* Q_f and R_f, it can be noted that the evolution of the value depends highly on the electrolyte used. Film capacity Q_f significantly decreases in the presence of $[Fe(CN)_6]^{3-/4-}$ from 8.2 μF s^{n-1} for non-infected RAW to 3 μF s^{n-1} for parasitized cells, whereas it increases from 6.3 to 11.7 μF s^{n-1} for LPS-stimulated macrophages. Conversely, this value is constant in the absence of probe. It can also be noted that R_f is constant with the probe, whereas it strongly decreases with infection or stimulation in the culture medium. All these comparisons suggest that interferences take place between the probe and the cell. The effect of ferricyanide $[Fe(CN)_6]^{3-}$ on macrophages has already been mentioned in the literature. Baoutina et al. (2001), for example, have demonstrated the capacity of macrophages to reduce *in vitro* transition metal such as Fe(III) by measuring the formation of ferrocyanide $[Fe(CN)_6]^{4-}$ from ferricyanide $[Fe(CN)_6]^{3-}$. The reduced transition metal ions generated (Fe(II)) might facilitate production of oxidative species *via* a Fenton-type reaction with the H_2O_2 produced. In the same way, Kaul et al. (1997) have demonstrated that ferricyanide, while this is not the case for ferrocyanide, is able to stimulate NF-kB *via* the redox reaction at the plasma membrane, NF-kB being the transcription factor that controls the inducible expression of a variety of genes, particularly those involved in inflammatory, immune, and acute-phase responses. The high value of Q_f recorded for healthy RAW with $[Fe(CN)_6]^{3-/4-}$ (8.2 μF s^{n-1}) could originate from morphological changes affecting the $[Fe(CN)_6]^{3-}$ stimulated cells as described in the literature for LPS-stimulated macrophages. Williams and Ridley (2000) have demonstrated on glass slides that LPS induced distinct changes in cell morphology and actin organization in monocytes and Bac1 mouse macrophage cells. These morphological changes are characterized by an increase in cell adhesion and spreading. As Q_f is proportional to the surface and inversely proportional to the film thickness, the high value obtained in the case of $[Fe(CN)_6]^{3-}$ stimulated RAW cells, could originate from an increase in film surface (cellular spreading) and/or to a decrease in cellular thickness, as illustrated in Scheme 1.

Taking into account modeling results, the ferricyanide effect on macrophages seems higher in healthy RAW cells than in parasitized ones. This result could be due to the fact, as described in the literature for LPS-activated cells, that infected cells take 40% longer to activate (Camacho et al., 2008). To summarize, in

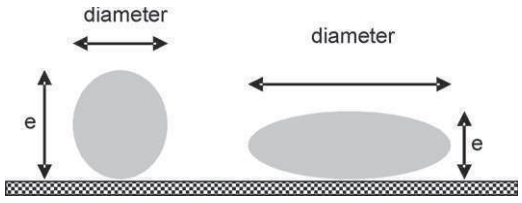

Scheme 1. Morphological changes that could affect RAW in the presence of $[Fe(CN)_6]^{3-}$.

Table 1
Modeling of EIS measurements performed on infected or stimulated macrophages using or not a redox probe. For EIS performed with the redox probe values of electrical components are deduced from the modeling of Nyquist diagrams (Figs. 1, 2a and b) according to the circuit model I. For EIS carried out without redox probe in the culture medium values of electrical components are deduced from the modeling of Nyquist diagrams (Fig. 2c and d) according to the circuit model II. The errors were obtained from the standard deviation.

		R_s (Ω)	Q_f ($\mu F s^{n-1}$)	n	R_f (Ω)	Q_{dl} ($\mu F s^{n-1}$)	n	R_{ct} (Ω)	σ_w ($\Omega s^{-1/2}$)
EIS performed with a redox probe	Bare gold	340 ± 10				3 ± 0.01	0.9 ± 0.01	300 ± 0	740 ± 50
	Uninfected	335 ± 8	8.2 ± 0.8	0.80 ± 0.02	72 ± 17	225 ± 3	0.55 ± 0.02	4500 ± 814	200 ± 73
	Leishmania parasitized	325 ± 10	3 ± 0	0.83 ± 0.01	77 ± 6	555 ± 110	0.53 ± 0.02	3170 ± 288	1630 ± 542
	Untreated	330 ± 1	6.3 ± 1.1	0.77 ± 0.02	93 ± 11	362 ± 16	0.55 ± 0.01	2633 ± 392	420 ± 67
	LPS-stimulated	335 ± 9	11.7 ± 2.9	0.73 ± 0.02	103 ± 25	322 ± 33	0.50 ± 0.02	4066 ± 230	471 ± 38
		R_s (Ω)	Q_f ($\mu F s^{n-1}$)	n	R_f (kΩ)	Q_{dl} ($\mu F s^{n-1}$)	n	R_{ads} (kΩ)	C_{ads} (μF)	R_{ct} (kΩ)	σ_w ($\Omega s^{-1/2}$)
EIS performed in the culture medium	Uninfected	460 ± 0	5.5 ± 0	0.88 ± 0.03	70 ± 4	2.6 ± 0.28	0.91 ± 0.03	725 ± 0	0.18 ± 0.03	650 ± 57	63 ± 29
	Leishmania parasitized	450 ± 3	6.0 ± 0.6	0.93 ± 0.017	10.0 ± 0.1	2.25 ± 0.05	0.89 ± 0.01	81.2 ± 0	0.1 ± 0	250 ± 1	107 ± 7
	Untreated	440 ± 30	5.5 ± 0	0.85 ± 0.03	150 ± 0	1.8 ± 0	0.91 ± 0.01	45 ± 7	0.15 ± 0.05	4000 ± 1400	500 ± 0
	LPS-stimulated	535 ± 21	5.25 ± 0.35	0.88 ± 0.05	50 ± 0	1.9 ± 0.54	0.91 ± 0.01	600 ± 26	0.15 ± 0.07	775 ± 176	80 ± 50

the case of *Leishmania*-infected cells, morphological changes are delayed by infection, and film capacity decreases with the infection, whereas in the case of LPS-stimulated macrophages the effects of $[Fe(CN)_6]^{3-}$ and LPS are combined inducing a great change in cell morphology, and thus an increase in film capacity. These opposed and cumulative morphological changes described for infected or LPS-stimulated macrophages, respectively, could also explain the different behaviors recorded for R_{ct}. R_{ct} decreases with the infection from 4500 to 3170 Ω, while it increases from 2633 to 4066 Ω in the case of LPS-stimulated RAW cells. The more swollen are the cells, the more insulating is the film, and the higher is the charge transfer resistance.

The stability of the film resistance in the case of experiments performed with a redox couple could also originate from interference between probe and cell. An activation of the macrophage by ferricyanide means that ions bind to the membrane as described for LPS in the case of LPS-activated RAW cells. Indeed, LPS binds to CD14 at the macrophage surface, then interacts with signaling receptor TLR4, toll-like receptors (TLRs) which recognize pathogen-associated molecular patterns and evoke various cell-signaling pathways (Moon and Pyo, 2007). Binding between the redox probe and the cell results in ion-intercalation in the cell membrane, *i.e.* in the cellular film itself, rendering the insulating properties independent of the cellular state, whether native or infected.

As far as the interface film/solution is concerned, in the case of impedance carried out with the redox probe, the imperfect capacity of double layer Q_{dl} increases for infected cells from 225 to 555 $\mu F s^{n-1}$, whereas it is stable for LPS-stimulated macrophages (~350 $\mu F s^{n-1}$). The increase in Q_{dl} recorded for parasitized macrophages toward normal ones could result from hyperpolarization of the cell membrane induced by the infection, as described by Forero et al. (1999).

Taking into account the huge effect of the redox probe on the healthy or even activated macrophages, electrochemical impedance spectroscopy using a probe is not adapted to the study of such cells.

For measurements performed in the culture medium, *i.e.* probe-free (Table 1), the first important change concerns film resistance R_f which decreases for infected and stimulated cells compared to healthy ones. These changes could originate from the *Leishmania* infection or LPS-activation mechanism leading to the release of a great number of reactive species including not only transient radical species such as $O_2^{\bullet -}$, $^{\bullet}OH$ and NO (Baoutina et al., 2001; Bhattacharya et al., 2008; Lemesre et al., 1997), but also calcium or potassium ions (Alexander et al., 1999; Bogdan et al., 1996) into the cellular layer. Several reports have indicated that LPS treatment can cause an increase in intracellular-free Ca^{2+} concentration which is associated with TNF-α production in alveolar macrophages and Kuffer cells (Chen et al., 1999; Zandi et al., 1997). It has also been shown that K^+ channels are involved in LPS-induced activation of macrophages (Haslberger et al., 1992; Lowry et al., 1998) and that, in murine macrophage J774.1 cells, LPS treatment changes the density of inwardly rectifying K^+ channels (McKinney and Gallin, 1990).

If most of the electrical components of the equivalent circuit vary in the same way for infected or LPS-stimulated cells, this is not the case for R_{ads} and R_{ct} which, respectively, characterize the production of electroactive species in the cellular layer or in the culture medium. These opposite variations result from the fact that these two stimuli induce diametrically contrary responses in RAW cells. Standard LPS macrophage activation leads to the production of inflammatory cytokines, reactive oxygen and nitrogen intermediates (ROIs and RNIs) among which nitric oxide produced endogenously and in great quantities by the inducible form of NO-synthase (iNOS), significantly expressed in LPS-activated macrophages. This highly diffusible radical is rapidly released from the cell. Moreover, the high concentration of nitric oxide in the cul-

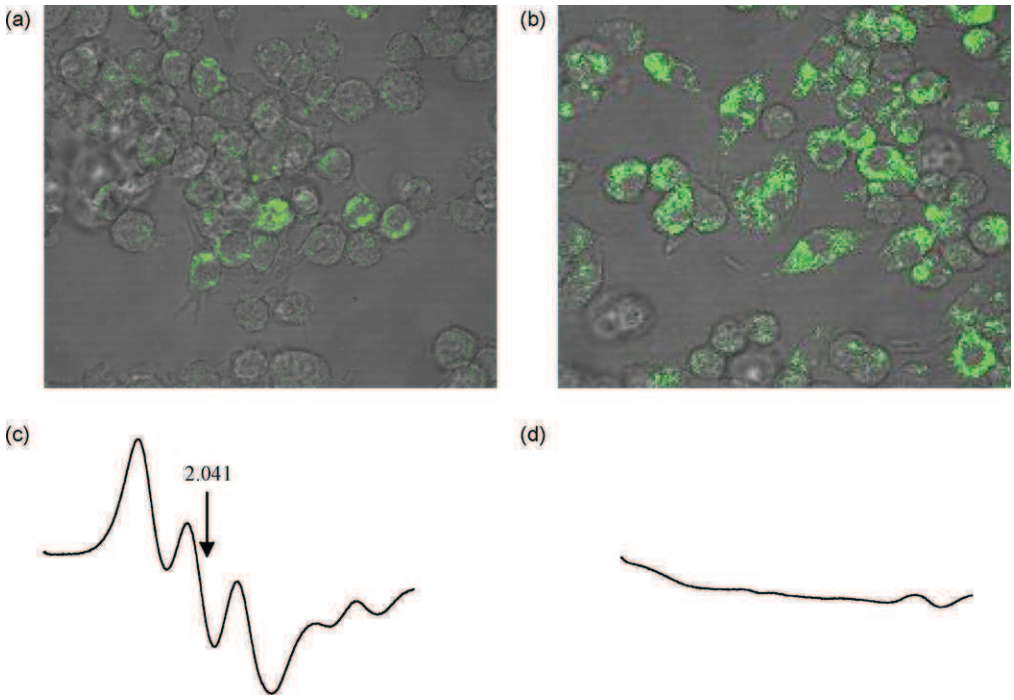

Fig. 3. Production of reactive species by *Leishmania*-infected or LPS-stimulated RAW cells. Image (63×) by confocal microscopy of RAW 264.7 cells after incubation with H_2DCFD recorded at 530 nm for (a) RAW 264.7 cells activated with LPS (1 μg/L) and (b) RAW 264.7 cells infected with *Leishmania amazonensis*. EPR spectra of the culture medium of RAW 264.7 cells recorded after 2 h of incubation with Fe(DETC)$_2$ for (c) macrophages activated with LPS (1 μg/L) and (d) macrophages infected with *Leishmania amazonensis*.

ture medium is responsible for the strong decrease of R_{ct} from 4000 to 775 kΩ following stimulation.

In the case of *Leishmania* infection, both *in vitro* and *in vivo* experimental models have demonstrated that leishmanicidal activity in murine macrophages is also mediated by reactive oxygen and nitrogen intermediates, especially NO (Jorens et al., 1995; Solbach and Laskay, 2000). However, to survive and multiply within the macrophage the parasite itself possesses mechanisms which may interfere with NO production (Perrella Balestieri et al., 2002). The decrease in NO produced in the case of *Leishmania*-infected cells compared to LPS-activated cells may explain the slighter decrease in charge transfer resistance R_{ct} from 650 to 250 kΩ. Conversely, the high decrease in R_{ads} from 725 to 81 kΩ recorded in this case could come from the production of lethal oxygen radicals by the cell in its cytosol (non-diffusible radicals) to eliminate invading pathogens (Mehta and Shaha, 2006).

In order to confirm the production of reactive oxygen species in the cell cytosol following infection by *Leishmania*, the production of oxygen-derived free radicals was measured with ROS fluorescent probe 2′,7′-dichlorodihydrofluorescein diacetate (DCF) using confocal microscopy. Non-ionized DCF is membrane-permeable and, therefore, diffuses readily into cells (Nasr-Esfahani et al., 1990). Confocal microscopic images of LPS-activated or *Leishmania*-infected macrophages carried out in the presence of DCF are presented in Fig 3a and b, respectively. These images clearly show a high fluorescent intensity in the infected cell (Fig. 3b) whereas this is not the case for LPS-stimulated macrophages (Fig. 3a), confirming that *Leishmania* induces a huge production of reactive oxygen species in RAW cells. In the same way, to confirm nitric oxide production in the case of LPS-stimulated macrophages and its diffusion outside the cell, electron paramagnetic resonance (EPR) was carried out using water-insoluble complex *N*,*N*-diethyldithiocarbamate [Fe(II)(DETC)$_2$] as a spin trap. Fig. 3c and d depicts X-band EPR culture-medium spectra of LPS-activated or *Leishmania*-infected RAW cells. Typical triple-line EPR spectra of [Fe(II)(NO)(DETC)$_2$] complex (a_N = 13.5 G, g = 2.041) was detected in the culture medium of LPS-stimulated RAW cells, confirming the presence in great quantities of nitric oxide radicals. Conversely, no triplet was detected for *Leishmania*-infected RAW cells, either in the supernatant (Fig. 3d), or in the cells (data not shown), confirming the ability of the parasite to interfere with NO production.

These results confirm our hypothesis of explaining variations in electric-component values (R_{ads}, R_{ct}), *i.e.* (i) a high production of diffusible NO radicals in the case of LPS-stimulated RAW, an NO production inhibited for *Leishmania*-infected cells and (ii) a high production of oxygen-reactive species within infected cells, whereas this production is not observed in LPS-stimulated ones.

4. Conclusions

These results are very promising since they demonstrate the ability of EIS to simply characterize in real time the oxidative stress generate by an infection. In particular it demonstrates its ability to discriminate between two diametrically opposite cell responses associated to two different stimuli, one caused by the internalization of a parasite, and the other by activation by a bacterium component. For further insight into the redox mechanisms discriminating cellular stress states, our aim now is to associate this device to complementary selective electrodes based on amperometric transduction for the determination of NO or $O_2^{\bullet -}$, for example.

Acknowledgments

Séverine Maurel-Chevalley deserves our deep gratitude for her technical assistance and knowledge of parasitology. We also thank *Université Paul Sabatier* and the *Institut de Recherche pour le Développement* for financial support.

References

Alexander, J., Satoskar, A.R., Russell, D.G., 1999. J. Cell Sci. 112, 2993–3002.
Arndt, S., Seebach, J., Psathaki, K., Galla, H.J., Wegener, J., 2004. J. Biosens. Bioelectron. 19, 583–594.
Asphahani, F., Zhang, M., 2007. Analyst 132, 835–841.
Baoutina, A., Dean, R.T., Jessup, W., 2001. FASEB J. 15, 1580–1582.
Bhattacharya, A., Biswas, A., Das, P.K., 2008. Free Radic. Biol. Med. 44, 779–794.
Bogdan, C., Gessner, A., Solbach, W., Röllinghoff, M., 1996. Curr. Opin. Immunol. 8, 517–525.
Camacho, M., Forero, M.E., Fajardo, C., Niño, A., Morales, P., Campos, H., 2008. Exp. Parasitol. 120, 50–56.
Chen, F., Castranova, V., Shi, X.L., Demers, L.M., 1999. Clin. Chem. 45, 7–17.
De Blasio, B.F., Laane, M., Walmann, T., Giaever, I., 2004. Biotechniques 36, 650–654.
Forero, M.E., Mariĩn, M., Corrales, A., Llano, I., Moreno, H., Camacho, M., 1999. J. Membr. Biol. 170, 173–180.
Gantt, K.R., Goldman, T.L., McCormick, M.L., Miller, M.A., Jeronimo, S.M., Nascimento, E.T., Britigan, B.E., Wilson, M.E., 2001. J. Immunol. 167, 893–901.
Giaever, I., Keese, C.R., 1984. Proc. Natl. Acad. Sci. 81, 3761–3764.
Haslberger, A., Romanin, C., Koerber, R., 1992. Mol. Biol. Cell 3, 451–460.
Jorens, P.G., Matthys, K.E., Bult, H., 1995. Med. Inflamm. 4, 75–89.
Kaul, N., Choi, J., Forman, H.J., 1997. Free Radic. Biol. Med. 24, 202–207.
Kondo, M., Osawa, T., Shibata, N., Kobayashi, M., Uchida, K., 2001. J. Biol. Chem. 277, 10459–10466.
Kowolenko, M., Keese, C.R., Lawrence, D.A., Giaever, I., 1990. J. Immunol. Methods 127, 71–77.
Lemesre, J.L., Sereno, D., Daulouède, S., Veyret, B., Brajon, N., Vincendeau, P., 1997. Exp. Parasitol. 86, 58–68.
Lowry, M.A., Goldberg, J.I., Belosevic, M., 1998. Clin. Exp. Immunol. 111, 597–603.
Luong, J.H., Habibi-Rezaei, M., Meghrous, J., Xiao, C., Male, K.B., Kamen, A., 2001. Anal. Chem. 73, 1844–1848.
Marx, K.A., Zhou, T., Montrone, A., McIntosh, D., Braunhut, S.J., 2005. Anal. Biochem. 343, 23–34.
McFadden, P., 2002. Science 297, 2075–2076.
McKinney, L.C., Gallin, E.K., 1990. J. Membr. Biol. 116, 47–56.
Mehta, A., Shaha, C., 2006. Free Radic. Biol. Med. 40, 1857–1868.
Moon, E.Y., Pyo, S., 2007. Immunol. Lett. 110, 121–125.
Mutsaers, S.E., Papadimitrou, J.M., 1988. J. Leukoc. Biol. 44, 17–26.
Nasr-Esfahani, M.H., Aitken, J.R., Johnson, M.H., 1990. Development 109, 501–507.
Nguyen, D.D., Huang, X., Greve, D.W., Domach, M.M., 2004. Biotechnol. Bioeng. 87, 138–144.
Otto, A.M., Brischwein, M., Motrescu, E., Wolf, B., 2004. Arch. Arch. Pharm. Pharm. Med. Chem. 337, 682–686.
Perrella Balestieri, F.M., Pires Queiroz, A.R., Scavone, C., Assis Costa, V.M., Barral-Netto, M., Abrahamsohn, I.D.A., 2002. Microbes Infect. 4, 23–29.
Pinsino, A., Della Torre, C., Sammarini, V., Bonaventura, R., Amato, E., Matranga, V., 2008. Cell Biol. Toxicol. 24, 541–552.
Ribaut, C., Reybier, K., Reynes, O., Launay, J., Valentin, A., Fabre, P.L., Nepveu, F., 2009. Biosens. Bioelectron. 24, 2721–2725.
Rider, T.H., Petrovick, M.S., Nargi, F.E., Harper, J.D., Schwoebel, E.D., Mathews, R.H., Blanchard, D.J., Bortolin, L.T., Young, A.M., Chen, J., Hollis, M.A., 2008. Science 301, 213–215.
Ritting, M.G., Bogdan, C., 2000. Parasitol. Today 16, 292–297.
Russell, D.G., 1995. Trends Cell Biol. 5, 125–128.
Solbach, W., Laskay, T., 2000. Adv. Immunol. 74, 275–317.
Stenger, D.A., Gross, G.W., Keeferb, E.W., Shaffera, K.M., Andreadisa, J.D., Maa, W., Pancrazio, J.J., 2001. Trends Biotechnol. 19, 304–309.
Stuehr, D.J., Marletta, M.A., 1987. Cancer Res. 47, 5590–5594.
Tiruppathi, C., Malik, A.B., Del Vecchio, P.J., Keese, C.R., Giaever, I., 1992. Proc. Natl. Acad. Sci. 89, 7919–7923.
Tlili, C., Reybier, K., Géloën, A., Ponsonnet, L., Martelet, C., Ben Ouada, H., Lagarde, M., Jaffrezic-Renault, N., 2003. Anal. Chem. 75, 3008–3012.
Williams, L.M., Ridley, A.J., 2000. J. Immunol. 164, 2028–2036.
Xiao, C., Lachance, B., Sunahara, G., Luong, J.H., 2002. Anal. Chem. 74, 1333–1339.
Xiao, C., Luong, J.H., 2005. Toxicol. Appl. Pharmacol. 206, 102–112.
Zandi, E., Rothwarf, D.M., Delhase, M., Hayakawa, M., Karin, M., 1997. Cell 91, 243–252.